مؤتمر الأزهر الهندسي الدولي العاشر

AL-AZHAR ENGINEERING
TENTH INTERNATIONAL CONFERENCE
December 24 - 26, 2008

Code: M 26

OPTIMAL LOCATION OF A HEAT SOURCE MOUNTED IN A SUBSTRATE COOLED BY NATURAL CONVECTION

R. K. Ali and K. M. El-Shazly
Faculty of Eng., Mech. Eng. Dept., Benha University,. Cairo, Egypt

ABSTRACT

In this paper a numerical investigation is carried out to determine the optimal location of a heat source mounted in a substrate in a cavity filled with a dielectric fluid of Pr = 25. The opposite vertical wall and the horizontal walls are assumed to be isothermal and adiabatic, respectively. The governing steady state partial differential equations for the fluid and solid regions are solved simultaneously using a control volume formulation. The heat source/fluid thermal conductivity fixed while the substrate/fluid thermal conductivity ratio is varied from 10 to 1000. The objective is to maximize the thermal conductance between the heat source and fluid that is equivalent to minimize the heat source temperature.

The predications show that the average Nusselt number of the heat source increases with increasing Rayleigh number and the decrease in heat source spacing from the cavity bottom surface. It is shown that increasing the substrate/fluid thermal conductivity ratio decreases the average heat source Nusselt number and increases its thermal conductance. For $Ra_b \le 10^7$, the optimum location is not critical with maximum thermal conductance at s/b=2.5. The optimal location migrates toward the lower corner of the cavity for $Ra_b > 10^7$ at $Rs < 100$ while it is critically at s/b=2.5 for $Rs \ge 100$. Numerical correlations for the average heat source Nusselt number and the thermal conductance as a function of Rayleigh number, heat source spacing from the cavity bottom surface and substrate/fluid thermal conductivity ratio were obtained.

© 2008 Faculty of Engineering, Al-Azhar University, Cairo, Egypt. All rights reserved.

KEYWORDS: NATURAL CONVECTION, NUMERICAL SIMULATION, THERMAL CONDUCTANCE, ELECTRONIC COOLING

Nomenclature

Symbols:

AR Aspect ratio , H/L
C heat source thermal conductance
b heat source height, m
g gravity acceleration
H cavity height, m
h heat transfer coefficient, w/m^2k
k thermal conductivity, w/m^2k
L cavity width, m
M number of nodes in x-direction
N number of nodes in y-direction
R Solid/fluid thermal conductivity ratio

Subscripts:

b based on the heat source height
local the local value
C the cold wall
f fluid
h heat source
L based on the cavity width
s substrate

p pressure, pa
q" heat flux, w/m^2
s heat source spacing from the cavity bottom surface, m
T temperature, k
u, v velocity components in x and y directions
w substrate width, m
X,Y dimensionless coordinate, x/b and y/b
x, y coordinate directions

Greek letters:

α thermal diffusivity
β volumetric thermal expansion coefficient of the fluid
φ stream function
θ dimensionless temperature
ρ density
ν kinematic viscosity
ζ refers to the solid/fluid thermal conductivity

Dimensionless terms*:*

Nu Nusselt number
Ra Rayleigh number
Pr Prandtl number

INTRODUCTION

The development of rather complex and highly dense electronic board necessitates the presence of very efficient cooling techniques. Current electronic stations use forced air convection to cool the computer chip surfaces. With increasing heat removal requirements, larger and powerful fans will be necessary for cooling purposes that associated with the noise and vibration problems. To eliminate these problems, natural convection provides an alternative cooling for these power systems. A major disadvantage to natural convection is that low heat transfer compared with forced convection. To perform higher-power dissipation level by using natural convection cooling scheme by mounting the electronic chips in a substrate and exposed to a the dielectric liquid. The coupling between the conduction in the substrate and convection to the fluid allows for thermal spreading to occur through the substrate and provides an additional heat transfer path from the heat source to the fluid. Wadsworth and Mudawar (1990) investigated through an experimental study the single phase heat transfer from a smooth simulated chip to a 2-D jet of dielectric liquid (FC-72) issuing from a thin rectangular slot into a channel confined between the chip surface and nozzle plate. Wang et al. (1997) investigated a natural convection air-cooling of a vertical plate with five wall-attached protruding discretely heated integrated circuit packages. Their study showed the influence of the blockage dimension and their power distribution on the buoyancy induced flow. Sultan (1999) studied experimentally the effect of aspect ratio on the mixed convection cooling of multiple protruding heat sources in a horizontal channel. Tewari and Jaluria (1990) presented an experimental study on the mixed convection from multiple heat sources mounted on horizontal and vertical surfaces. Their study showed the effect of separation distance on heat transfer from the components. Papanicolaou and Jaluria (1990) studied numerically the mixed convection heat transfer from a single flush mounted heat source located in an

enclosure for $50< Re<2000$ and $0< Gr/Re^2<10$. Icoz et al. (2007) designed air and liquid cooling systems for electronic components using concurrent simulation and experiment. Oscillations is a common phenomena encountered in electronic cooling applications. Wang and Jaluria (2002) and Kim et al. (1998) found that inducing oscillations in the driving flow enhances the heat transfer rates from the heat sources. Nigen and Amon (1994) and Lin and Lin (1996) studied in detail the stability and self-sustained oscillations. Icoz and Jaluria (2004) presented a methodology for the design and optimization of cooling systems for electronic equipment. They studied the mixed convection flow in a horizontal and a vertical channels with isolated electronic components on the walls. Heindel et al. (1995) studied numerically coupled conduction and natural convection transport within discretely heated cavity filled with a dielectric fluid (FC-77). They studied the effect of Rayleigh number and the substrate/fluid thermal conductivity ratio on the maximum interface temperature. Heindel et al. (1996) investigated numerically and experimentally a single phase natural convection heat transfer for an array of highly-finned discrete heat sources mounted to one wall of cavity filled with dielectric liquid (FC-77). They found that finned surfaces enhances heat transfer by as much as a factor of 24. Fujii et al. (1996) carried out a numerical and experimental study on natural convection heat transfer to air from an array of vertical parallel plates with protruding and discrete heat sources. A correlation expression for local Nusselt number and a method for estimating the maximum inner temperature of the heat sources are proposed, and the thermally optimum spacing of the parallel plates is discussed. Yu and Joshi (1997) presented a 3-D numerical investigation of steady laminar natural convection from a discrete flush-type heat source mounted on the substrate in vented enclosure. They presented local and overall heat transfer from the heat source and the substrate in terms of Nusselt numbers and surface temperatures to illustrate vent effects. Silva et al. (2005) used the constructal method to determine the optimum distribution and sizes of bare discrete heat sources in a vertical open channel cooled by natural convection. Tito and Luiz (2006) applied genetic algorithms to study the optimal location of bare heat sources on a vertical wall cooled with natural convection. Silva et al. (2004) studied analytically and numerically the optimal distribution of discrete heat sources on a horizontal plate cooled with laminar forced convection. This study showed that the heat sources should be placed non-uniformly on the wall and near the tip of the boundary layer. Silva et al. (2006) presented the optimal distribution of a bare discrete heat sources mounted in i) a vertical wall ii) on a side wall of a 2-D enclosure iii) on the wall of a vertical diverging or converging channel with chimney flow. Their numerical simulations show that for maximum heat transfer rate density it is better to install heated sources at the channel entrance and the angle between the walls is approximately zero for larger Rayleigh number. Silva et al. (2004) applied the constructal method to discovery the optimal distribution of line discrete heat sources on a vertical wall or mounted on a wall of a 2-D enclosure. Their study showed that the optimal distribution is not uniform and as Rayleigh number increases the heat sources should be placed near the tip of the boundary layer. As can be seen, several papers have been published on the heat transfer performance of a wall with distributed bare heat sources. In the present study we consider the fundamental problem of optimal location of a heat source mounted in a substrate on a vertical wall of a 2-D enclosure filled with a dielectric liquid (FC-77). The global objective is to maximize the conductance between the heat source and the fluid that equivalent to minimize the temperature of the heat source. The local and overall heat transfer from the heat source and the substrate in terms of Nusselt numbers and the surface temperatures are presented to illustrate the Rayleigh number and the substrate/fluid thermal conductivity ratio. .

Governing Equations

The configuration under study is shown in Fig. 1. One vertical wall of the cavity is composed of heat source mounted in a substrate to simulate an electronic chip. An isoflux is applied on the back of the heat source while the back of the substrate is adiabatic. An isothermal boundary condition is maintained at the opposing wall and the horizontal walls are assumed to be adiabatic. The thermo-physical properties of the source, substrate and the fluid are assumed to be constant but different. Assuming 2-D steady-state heat transfer laminar natural convection with no viscous dissipation governing equations for the fluid and solid regions can be written as follows:

Fluid:

Continuity: $$\frac{\partial \mathrm{U}}{\partial \mathrm{X}}+\frac{\partial \mathrm{V}}{\partial \mathrm{Y}}=0 \tag{1}$$

X-momentum: $$\mathrm{U}\frac{\partial \mathrm{U}}{\partial \mathrm{X}}+\mathrm{V}\frac{\partial \mathrm{U}}{\partial \mathrm{Y}}=\mathrm{Pr}\left(\frac{\partial^2 \mathrm{U}}{\partial \mathrm{X}^2}+\frac{\partial^2 \mathrm{U}}{\partial \mathrm{Y}^2}\right)-\frac{\partial \mathrm{P}}{\partial \mathrm{X}} \tag{2}$$

Y-momentum: $$U\frac{\partial V}{\partial X}+V\frac{\partial V}{\partial Y}=\mathrm{Pr}\left(\frac{\partial^2 V}{\partial X^2}+\frac{\partial^2 V}{\partial Y^2}\right)-\frac{\partial P}{\partial Y}+Ra_b\,\mathrm{Pr}\,\theta \tag{3}$$

Energy: $$\mathrm{U}\frac{\partial \theta}{\partial \mathrm{X}}+\mathrm{V}\frac{\partial \theta}{\partial \mathrm{Y}}=\frac{\partial^2 \theta}{\partial \mathrm{X}^2}+\frac{\partial^2 \theta}{\partial \mathrm{Y}^2} \tag{4}$$

Solid:

Energy:

$$0=\zeta\left(\frac{\partial^2 \theta}{\partial X^2}+\frac{\partial^2 \theta}{\partial Y^2}\right) \tag{5}$$

Where:

$$\mathrm{X}=\frac{\mathrm{x}}{\mathrm{b}} \qquad \mathrm{Y}=\frac{\mathrm{y}}{\mathrm{b}} \tag{6}$$

$$\mathrm{U}=\frac{\mathrm{u}}{(\alpha_\mathrm{f}/\mathrm{b})} \qquad \mathrm{V}=\frac{\mathrm{v}}{(\alpha_\mathrm{f}/\mathrm{b})} \tag{7}$$

$$P=\frac{p}{\rho(\alpha_f/b)^2} \qquad \theta=\frac{T-T_C}{(q^{"}.b/k_f)} \tag{8}$$

$$\mathrm{Pr}=\frac{\upsilon}{\alpha_f} \qquad Ra_h=\frac{g\beta q^{"}b^4}{(k_f\alpha_f\upsilon)} \tag{9}$$

$$R_s=\frac{k_s}{k_f} \qquad R_h=\frac{k_h}{k_f} \qquad \zeta=\begin{cases}R_s & in\ \ the\ \ substrate\ \ region\\ R_h & in\ \ the\ \ heater\ \ region\end{cases} \tag{10}$$

The boundary condition to the above equations are as follows:

At X = 0 V=U=0 $$\frac{\partial \theta}{\partial \mathrm{X}}=\begin{cases}\dfrac{-1}{\mathrm{R_h}} & \text{at the heater region}\\ 0 & \text{at the substrate region}\end{cases} \tag{11}$$

At X = L/b V=U=0 $$\theta=0 \tag{12}$$

At Y = 0 V=U=0 $$\frac{\partial \theta}{\partial \mathrm{Y}}=0 \tag{13}$$

At Y = H/b V=U=0 $$\frac{\partial \theta}{\partial \mathrm{Y}}=0 \tag{14}$$

The heat fluxes and the temperatures at interfaces of dissimilar materials is implicitly effected through the harmonic mean formulation of the interfaces thermal conductivities.

Numerical Approach

The governing partial differential equations for the conjugate problem were discretized on uniform dense grid using control volume formulation employing the simpler algorithm detailed in Patankar (1980). The changes of thermal conductivity at the interface of solid/fluid or solid/solid are handled by he harmonic mean formulation presented by Patankar (1980). However, separate equations were written for the fluid and solids regions, numerical results are obtained in both regions simultaneously by solving the continuity, momentum and energy equations in the entire domain. The numerical solution is considered to be converged when the relative change in the temperature and the velocity of order 10^{-5} and 10^{-4}, respectively. The present predictions were validated by solving for a 2-D natural convection in an isothermal and isoflux heated cavity. The adequacy of grids within isothermal heated enclosure was tested for $\mathrm{Ra_L} = 10^6$ and AR=4 and the results are shown in Table1. Most of the numerical runs were performed using grid M x N of 50x194 at $\mathrm{Ra_L} = 10^4$ and up to 242x194 at $\mathrm{Ra_L} = 10^9$ for H/b=8, L/b=2 and w/b=0.5.

Results and Discussions

The validity of the present model was performed for isothermal and isoflux heated cavity as shown in Fig.2. A good agreement was found between the present predictions and the following correlations presented in Incroperia and DeWitt (1990).

i) for isothermal heated cavity:

$$Nu_L = 0.22\left(\frac{\mathrm{Pr}}{0.2+\mathrm{Pr}}Ra_L\right)^{0.28}\left(\frac{H}{L}\right)^{-0.25}, \qquad \left\{\begin{array}{l} 2 < \frac{\mathrm{H}}{\mathrm{L}} < 10, \qquad \mathrm{Pr} < 10^5 \\ 10^3 < \mathrm{Ra_L} < 10^{10} \end{array}\right\} \quad (15)$$

ii) for isoflux heated cavity:

$$\mathrm{Nu_L} = 0.24(\mathrm{Ra_L})^{0.25}\,\mathrm{Pr}^{0.012}\left(\frac{\mathrm{H}}{\mathrm{L}}\right)^{-0.5}, \qquad \left\{\begin{array}{l} 10 < \frac{\mathrm{H}}{\mathrm{L}} < 40, \qquad 1 < \mathrm{Pr} < 2\mathrm{x}10^4 \\ 10^4 < \mathrm{Ra_L} < 10^7 \end{array}\right\} \quad (16)$$

The relative error for the average Nusselt number between the present predictions and these correlations is within 11%. Many numerical runs were performed to study the effect of Rayleigh number and the substrate/fluid thermal conductivity ratio on the local and overall heat transfer rates from the heat source and the substrate and to obtain the optimal location of the heat source. The optimal location of the heat source was determined by maximizing the thermal conductance of the heat source that equivalent to minimizing the temperature of the hot spot on the heat source, namely:

$$C = \frac{q''}{k_h(T_{\max} - T_C)/b} \qquad (17)$$

The thermal conductance is a dimensionless way of expressing the ratio of total heat transfer (Q=q" x b) divided by the largest temperature difference between the heat source and the cold wall as discussed in Silva et al.(2004, 2004 and 2006)

Rayleigh number effect

The effect of Rayleigh number, Ra_b, variation due to the applied heat flux on the flow field is shown in the streamlines and isotherms of Fig. 3. At $Ra_b = 10^4$, the flow field is weak with $|\varphi_{max}| = 9.8$ and unicellular as displayed in Fig. 3a. A thick boundary layer and a small stagnant core above the center of cavity are displayed. Increasing Ra_b thins the boundary layer that is characterized by large velocity and enlarges the stagnant core regions. This trend is shown in Fig. 3b for $Ra_b = 10^9$ with $|\varphi_{max}| = 170.25$. This is displayed by closely spaced streamlines that appear as a thick band at the interface. The great portion of the fluid descending along the cold wall is swept toward the leading edge of the heater zone. Figure 3c shows the non-dimensional isotherms in solid and the fluid regions at $Ra_b = 10^4$. The predicted almost vertical isotherms indicate the heat transfer in fluid zone is dominated by conduction mode. With increasing Ra_b, the central zone of the fluid is completely stratified and the thermal boundary layer at the hot and cold walls are extremely thin. The heater face is isothermal ($\theta_{heater} = 0.14$ at $Ra_b = 10^4$ and $\theta_{heater} = 0.022$ at $Ra_b = 10^9$) due to the high thermal conductivity of the heater. The actual average heater temperature increases with Ra_b because the increase in energy transferred to the enclosure as the heat flux increases. However, the average dimensionless temperature decreases because of the definition of $\theta = \frac{T - T_C}{q''b/k_f}$ where the increase in T-T_C is not commensurate with the corresponding increase in q. The effect of Rayleigh number on the local dimensionless temperature along the solid/fluid interface is shown in Fig. 4 for $Ra_b = 10^4$ to 10^9. The interface temperature increases from the cavity bottom to the heater leading edge and display isothermal along the heater face due to the higher thermal conductivity of the heater. At the trailing edge of the heater, the thermal boundary layer diminishes and the substrate/fluid interface temperature decreases monotonically. The dimensional temperature increases with Ra_b while its non-dimensional values decreases due to its definition. The dimensionless local heat flux at the solid/fluid is shown in Fig. 5 for $Ra_b = 10^4$ to 10^9. The largest value of dimensionless heat flux occurs at the leading edge and increases with the increase in Ra_b caused by thinning the thermal boundary layer and consequently the local Nusselt number. The opposite behavior of the dimensionless heat flux was noticed in the substrate region due to the reduced in the thermal spreading. The variation in Nu_{Local} is shown in Fig.6 for the full studied range of Rayleigh number. The local Nusselt number increases with increasing Ra_b caused by thinning of the thermal boundary layer. In all cases, a local spike exists at the leading edge of the heater. This is due to the advection occurred at the heater edge and the stream-wise conduction. Also, a second smaller peak at the trailing edge of the heater was found due to the stream-wise in the substrate and the small portion of the advection at the trailing edge. The average Nusselt number of the heat source as a function of Ra_b for different values s/b is displayed in Fig. 7. For a fixed Ra_b, the heat source average Nusselt number increases with the decrease in s/b because of the thinner thermal boundary at lower locations. Figure 8 shows how the thermal conductance varies with the position of the heat source in the substrate when Rayleigh number is varied due to the applied power. The optimal location is the one in which the heat source is located associated with higher conductance. For $Ra_b < 10^7$, the optimum location is not critical because the conductance distribution is almost

flat with maximum at s/b=2.5. The optimal location migrates toward the lower corner of the cavity for $Ra_b \geq 10^7$ where the minimum thickness of the thermal boundary layer.

Substrate/fluid thermal conductivity ratio effect

The effect of substrate/fluid thermal conductivity ratio, R_S, on the flow and thermal characteristics was examined for $10 < R_S < 1000$. Figure 9 shows streamlines and isotherms for two different substrate/fluid thermal conductivity ratios at $Ra_b = 10^4$. Increasing R_S causes the core descends toward the center of the cavity. The flow pattern at R_S=1000 is typical of that associated with a differentially heated cavity. Isotherms for these conditions are presented in Fig. 9 (c and d). The maximum dimensionless temperature decreases with increasing R_S and uniform temperature distribution in the solid zone (heater and substrate) is obtained. This is due to the increase in the thermal spreading in the substrate before transferring to the fluid. At R_S =1000, the fluid isotherms are typical of that associated with a differentially heated cavity and nearly uniform temperature distribution along the solid/fluid interface due to the increase in the substrate thermal conductivity as shown in Fig. 10. The thermal conductance of the heat source increases with the increase in the substrate/fluid thermal conductivity ratio as more thermal spreading occurs through the substrate as displayed Fig. 11. However, increasing R_S from 10 to 1000, the heat source location is not critically for $Ra_b \leq 10^7$ with optimum at s/b=2.5. For $Ra_b > 10^7$, the optimum location is critically at s/Lh=2.5 for $R_S \geq 100$ and migrates at the lower corner for $R_S < 100$. The effect of substrate/fluid thermal conductivity ratio on the average Nusselt number of the heater surface is noticeable for higher Rayleigh number as shown in Fig. 12. It can be seen that at a fixed Rayleigh number, the heater average Nusselt number decreases with the increase in R_S. This is due to the reduction in buoyancy effect and the decline in the fluid circulation related to the decrease in the fluid element temperature (T_f -T_C) as R_S increases. Also, increasing R_S increases the conduction through the substrate below the heater. Therefore, preheating the fluid below the heater is performed that decreases the heat removal rate at the heater surface. The Nusselt number and the thermal conductance of the heat source were correlated using the numerical data as,

$$Nu_b = 0.2467\, Ra_b^{0.2321} \left(\frac{s}{b}\right)^{-0.04956} R_s^{-0.11} \tag{18}$$

and

$$C = 2.09\, Ra_b^{0.1744} \left(\frac{s}{b}\right)^{-0.06078} \left(\frac{R_S}{R_S - 0.013}\right)^{-394.8} \tag{19}$$

Correlation (18 and 19) are valid for $10^4 < Ra_b \leq 10^9$, $0.5 \leq s/b \leq 5.5$ and $10 \leq R_S \leq 1000$ with maximum deviations for the Nusselt number and the thermal conductance of 21% and 16%, respectively. Figure 13 (a and b) shows the correlated values versus the numerical data for the Nusselt number and the thermal conductance of the heat source within the investigated ranges of the different parameters. A good agreement between the correlations and numerical data at R_S =100 and s/b=2.5 was obtained as shown in Fig. 14

CONCLUSIONS

In this paper we considered the problem of how to locate a heat source mounted in a substrate on a vertical side of closed cavity filled with a dielectric liquid (FC-77). The effect of Rayleigh number and the substrate/fluid thermal conductivity on the flow and thermal characteristics were numerically studied. At small values of Rayleigh number ($Ra_b \approx 10^4$), the heat transfer in the cavity is dominated by conduction. With increasing Ra_b, the central zone of the fluid is completely stratified and uniform heater temperature is obtained. The average Nusselt number of the heat source increases with increasing Rayleigh number and the decrease in heat source spacing from the cavity bottom surface. For $Ra_b < 10^7$, the optimum location is not critical with maximum conductance at s/b=2.5 while the optimal location migrates toward the lower corner of the cavity for $Ra_b \geq 10^7$. Increasing solid/fluid thermal conductivity decreases the maximum dimensionless temperature and a uniform temperature distribution in the solid zone. The average heater Nusselt number decreases as substrate/fluid thermal conductivity ratio increases. In general, the increase in substrate/fluid thermal conductivity ratio increases the conductance heater. For $Ra_b > 10^7$, the optimum location is critically at s/b=2.5 for $R_S \geq 100$ and migrates at the lower corner for $R_S < 100$. Numerical correlations for the average heat source Nusselt number and the thermal conductance as a function of Rayleigh number, heat source spacing from the cavity bottom surface and substrate/fluid thermal conductivity ratio were obtained

REFERENCES

1. da Silva A.k., Lorente S. and Bejan A., 2004., "Optimal distribution of Discrete Heat Sources on a Plate with Laminar Forced Convection ", Int. J. Heat and Mass Transfer ,Vol. 47, pp. 2139-2148.
2. da Silva A.k., Lorente S. and Bejan A., 2005., "Distribution of Heat Sources in Vertical Open Channels with Natural Convection ", Int. J. Heat and Mass Transfer ,Vol. 48, pp. 1462-1469.
3. da Silva A.k., Lorente S. and Bejan A., 2006., "constructal Multi-Scale Structures for Maximal Heat Transfer Density", Energy ,Vol. 31, pp. 620-635.
4. da Silva A.k., Lorenzini G. and Bejan A., 2004, "Distribution of Heat Sources in Vertical Open Channels with Natural Convection", Int. J. Heat and Mass Transfer ,Vol. 47, pp. 203-214.
5. Fujii M., Gima S., Tomimura T. and Zhang X., 1996, "Natural Convection to Air from an Array of Vertical Parallel Plates with Discrete and Protruding Heat Sources ", Int. J. Heat and Fluid Flow, Vol. 17, pp. 483-490.
6. Heindel T.J., Incropera F.P. and Rmadhyani S., 1995, "Conjugate Natural Convection from an Array of Disrete Heat Sources: Part 2- A Numerical Parametric Study", Int. J. Heat and Fluid Flow ,Vol.16, No. 6, pp. 511-518.
7. Heindel T.J., Incropera F.P. and Rmadhyani S., 1996, "Enhancement of Natural Convection Heat Transfer from an Array of Discrete Heat Sources", Int. J. Heat and Mass Transfer ,Vol. 39, No. 3, pp. 479-490.
8. Icoz T. and Jaluria Y., 2004 "Design of Cooling Systems for Electronic Equipment Using Both Experimental and Numerical Inputs" Journal of Electronic Packaging (ASME Transactions), Vol. 126, pp. 465–471.
9. Icoz T., Verma N. and Jaluria Y., 2007, "Design of Air and Liquid Cooling Systems for Electronic Components Using Concurrent Simulation and Experiment", Journal of Electronic Packaging (ASME Transactions) Vol. 128 ,pp. 466–478.

10. Incropera F.P. and DeWitt D.P., 1990, "Fundamentals of Heat and Mass Transfer ", John Wiley & Sons, New York.
11. Kim S. Y., Kang B. H., and Jaluria Y., 1998, "Thermal Interaction Between Isolated Heated Electronic Components in Pulsating Channel Flow", Numer. Heat Transfer, Part A, 34, pp. 1–21.
12. Lin W. L., and Lin T. F., 1996, "Experimental Study of Unstable Mixed Convection of Air in a Bottom Heated Horizontal Rectangular Duct", Int. J. Heat Mass Transfer, Vol. 39No. 8, pp. 1649–1663.
13. Nigen, S.J., and Amon, C. H., 1994, "Time-Dependent Conjugate Heat Transfer Characteristics of Self-Sustained Oscillatory Flows in a Grooved Channel", ASME J. Fluids Eng., 116, pp. 499–507.
14. Papanicolaou E. and Jaluria, Y., 1990, "Mixed Convection From an Isolated Heat Source in a Rectangular Enclosure", Numer. Heat Transfer, Part A, Vol. 18, pp. 427–461.
15. Patankar, S.V., 1980 "Numerical Heat Transfer and Fluid Flow ", Hemisphere publishing, Bristol, PA
16. Sultan G.I., 1999, "Mixed convecton cooling of multiple protruding heat sources in a horizontal channel", Mansoura Engineering Journal Vol. 24, No. 3, pp. 43–53.
17. Tewari, S. S., and Jaluria, Y., 1990, "Mixed Convection Heat Transfer From Thermal Sources Mounted on Horizontal and Vertical Surfaces," ASME J. Heat Transfer, 112, pp. 975–987.
18. Tito D.Jr., and Luiz F.M., 2006., "Optimal Location of Heat Sources on a Vertical Wall with Natural Convection Through Gentetic Algorithms ", Int. J. Heat and Mass Transfer ,Vol. 49, pp. 2090-2096.
19. Wadsworth D.C. and Mudawar I., 1990, "Cooling of a multi-electronic module by means of confined two-dimensional jets of dielectric liquid", Journal of Heat Transfer (ASME Transactions) Vol. 112, pp. 891–898.
20. Wang H.Y., Penot F. and Sauliner A., 1997, "Numerical study of a buoyancy induced flow
21. along a vertical plate with discretely heated integrated circuit packages", Int. Journal of Heat and Mass Transfer Vol. 40 No. 7, pp. 1509–1520.
22. Wang, Q., and Jaluria, Y., 2002, "Unsteady Mixed Convection in a Horizontal Channel With Protruding Heating Blocks and a Rectangular Vortex Promoter", Phys. Fluids, Vol. 14, pp. 2109–2112.
23. Yu E. and Joshi Y., 1997, "A Numerical Study of Three-dimensional Laminar Natural Convection in a Vented Enclosure ", Int. J. Heat and Fluid Flow, Vol. 18, pp. 600-612.

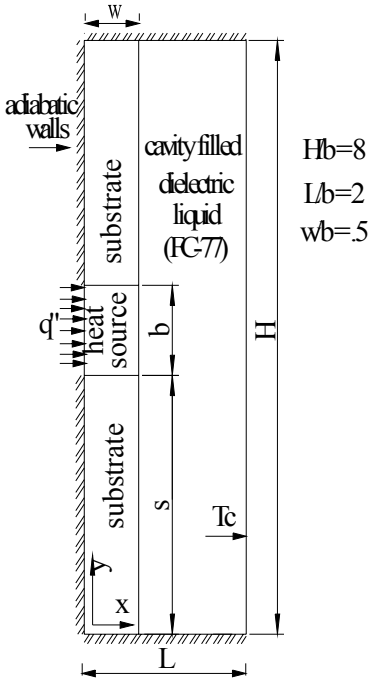

Fig. 1 : Schematic of the cavity with a heat source mounted in a substrate and an opposing isothermal wall

Tabel 1 : Grid Test for isothermal heated enclosure at $Ra_L=10^4$, AR=4

Grid (M x N)	15 x 30	25 x 50	43 x 98	87 x 172	87 x 350	172 x 350
Nu_L	8.7	7.5	7.3	7	7	6.9

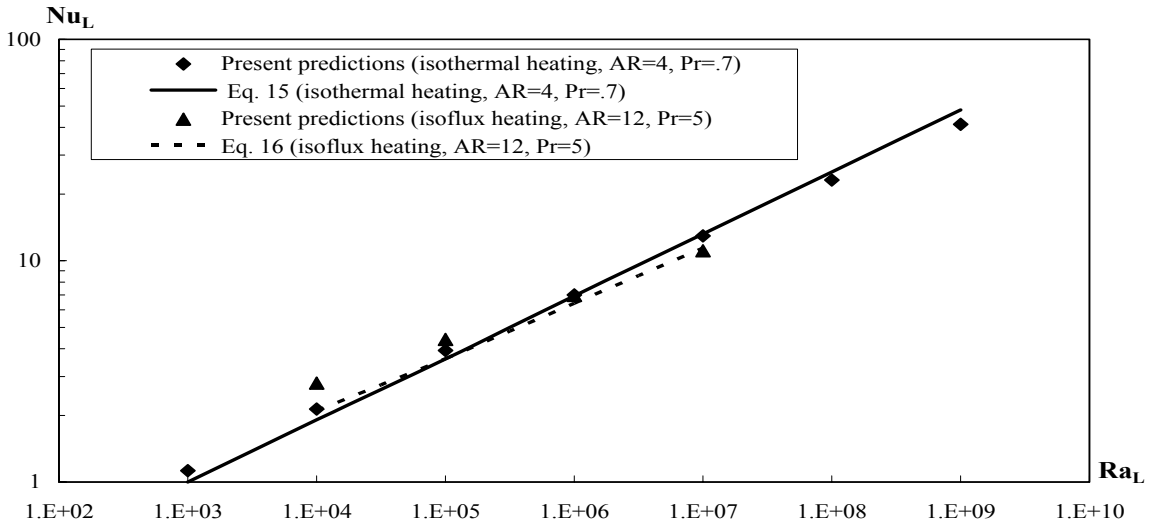

Fig. 2: Comparison of the present predictions data with the correlations presened in Incroperia and DeWitt (1990) for isothermal and isoflux heated cavity (1.E+09=10^9)

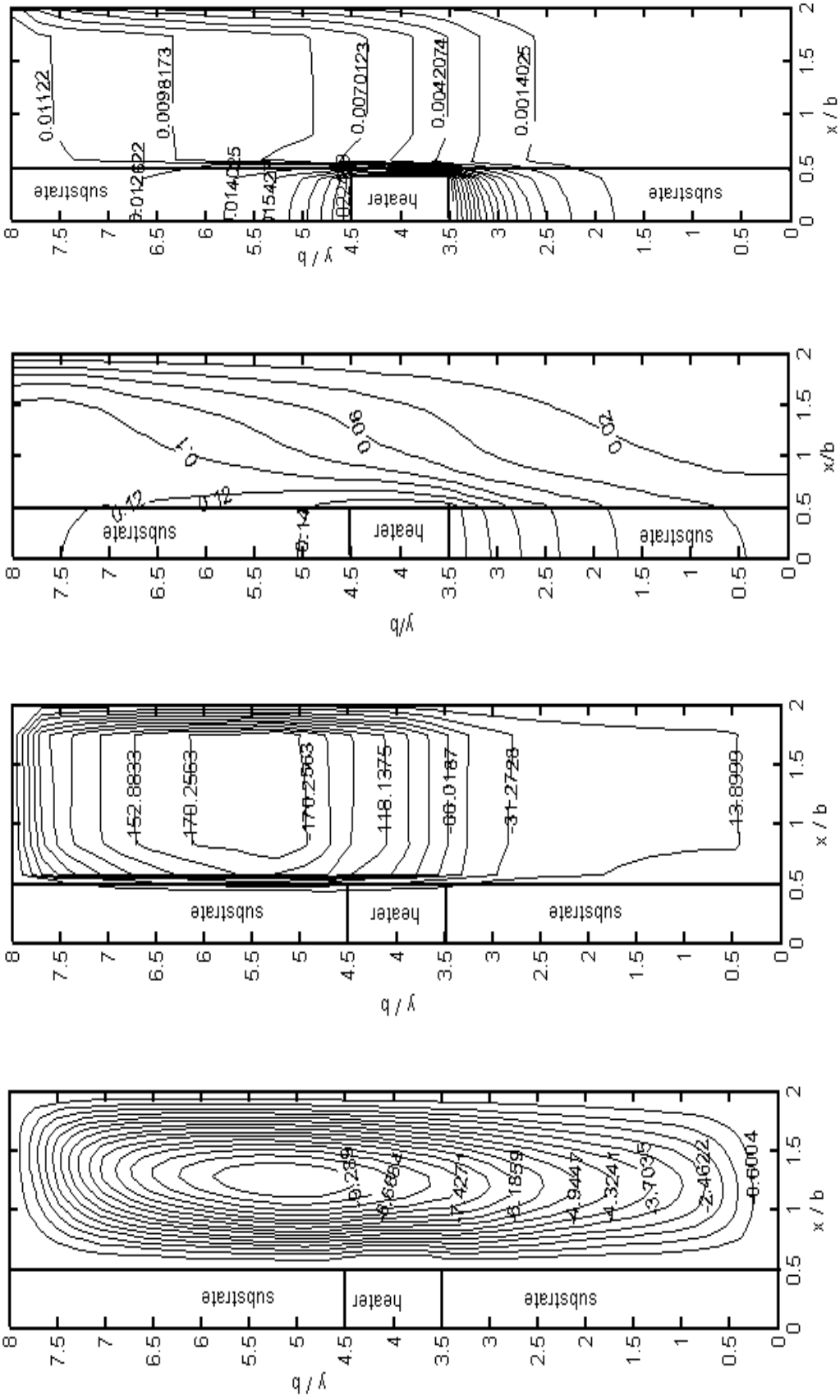

Fig. 3: Dimensionless streamlines (a: $Ra_b=10^4$ b: $Ra_b=10^9$) and isotherms (c: $Ra_b=10^4$ d: $Ra_b=10^9$) for Pr=25, R_s=10, s/b=3.5 and R_h=2350

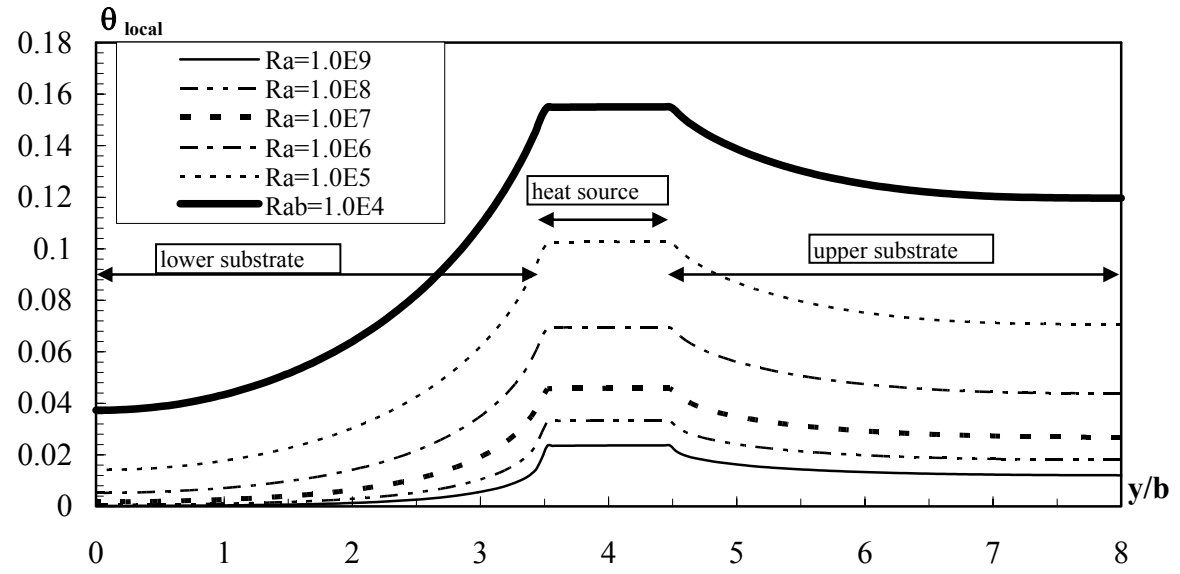

Fig: 4 Effect of Rayleigh number on the local dimensionless temperature profiles at the solid/fluid interface for Pr=25, R_s=10 and R_h=2350 (Ra refers to Ra_b and 1.0E9=10^9)

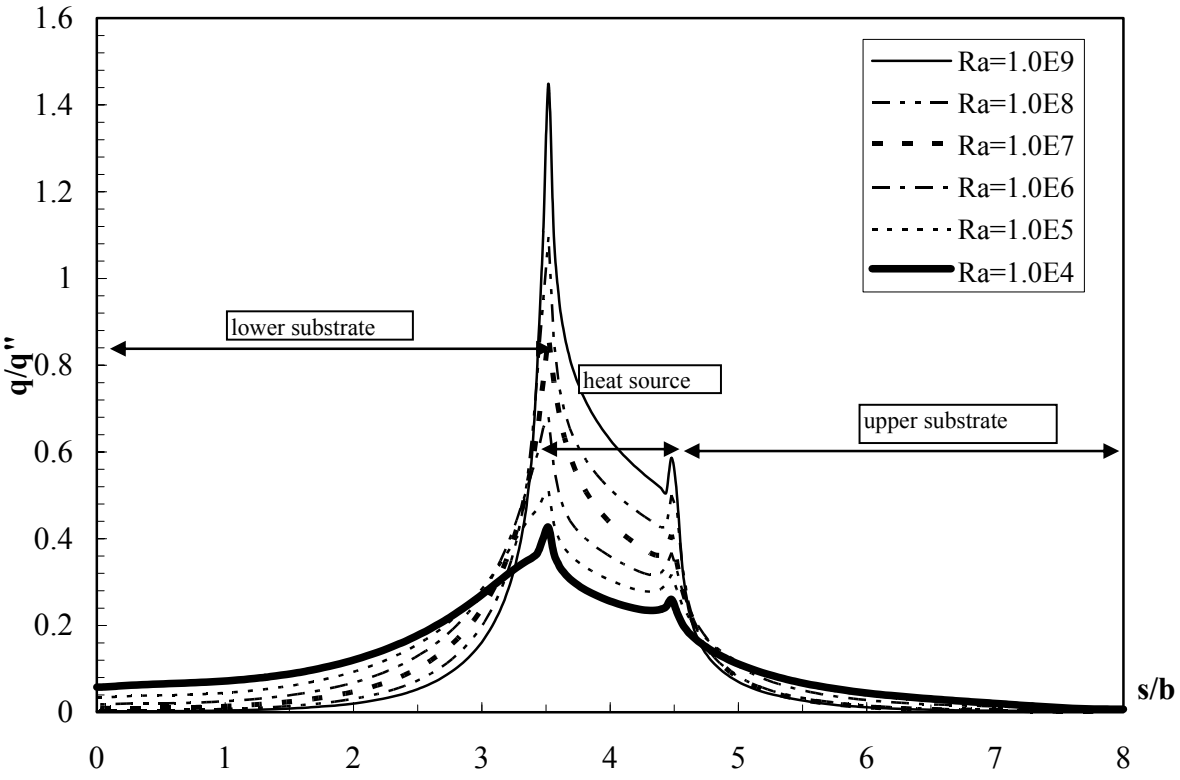

Fig: 5 Effect of Rayleigh number on the local dimensionless heat flux at the solid/fluid interface for Pr=25, R_s=10 and R_h=2350 (Ra refers to Ra_b)

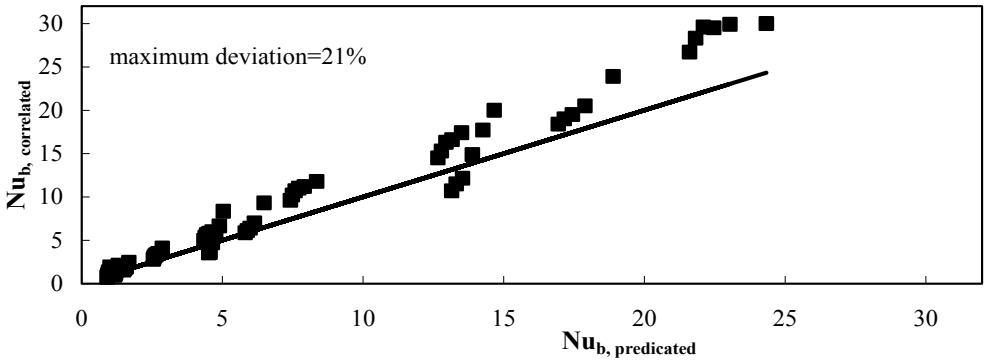

a) For Nussult number of heat source

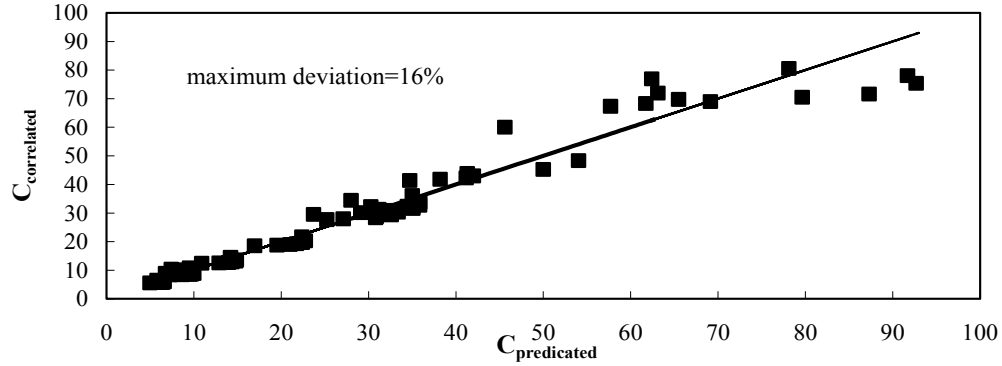

b) For the thermal conductane of the heat source

Fig. 13: Correlated values versus numerical data

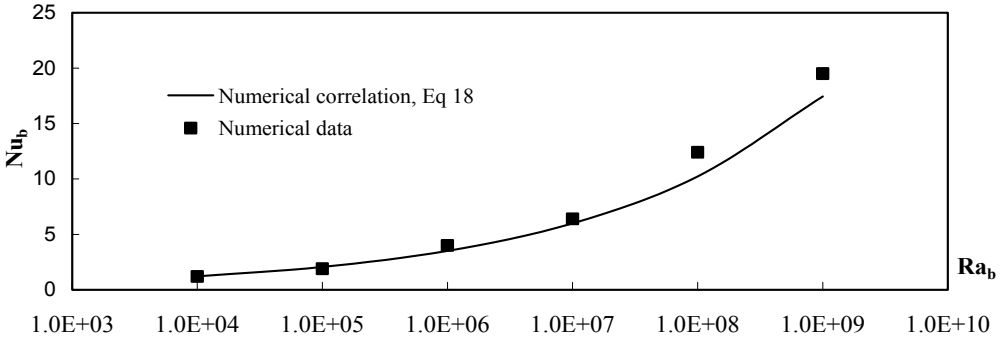

a) For Nussult number of heat source

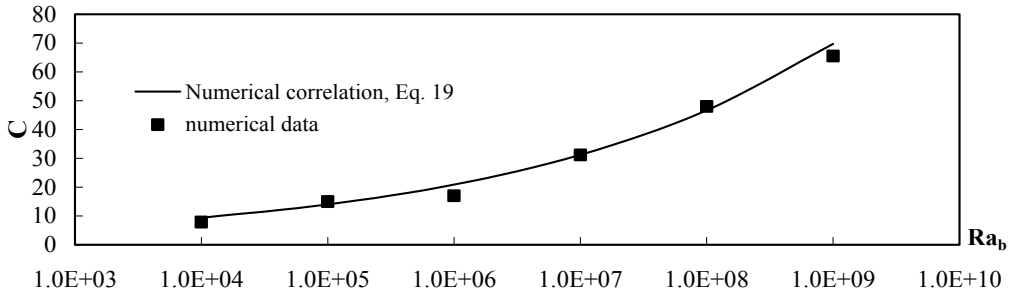

b) For the thermal conductane of the heat source

Fig.14: Comparison between the obtained correlations and present numerical data at s/b= and R_s=100